2023 年臺灣國際科學展覽會
優勝作品專輯

作品編號 **180019**

參展科別 **地球與環境科學**

作品名稱 **Evaluation of a fiber optic distributed temperature measurement system for a geothermal energy**

得獎獎項 **一等獎**

國　　家 **Switzerland**

就讀學校 **Lycée Denis de Rougemont, Neuchâtel**

指導教師

作者姓名 **Loic Posta**

關鍵詞 **Geothermal、Heat Storage、Distributed Temperature Sensing (DTS) by optic fiber (Distributed Temperature Measurement System)**

作者照片

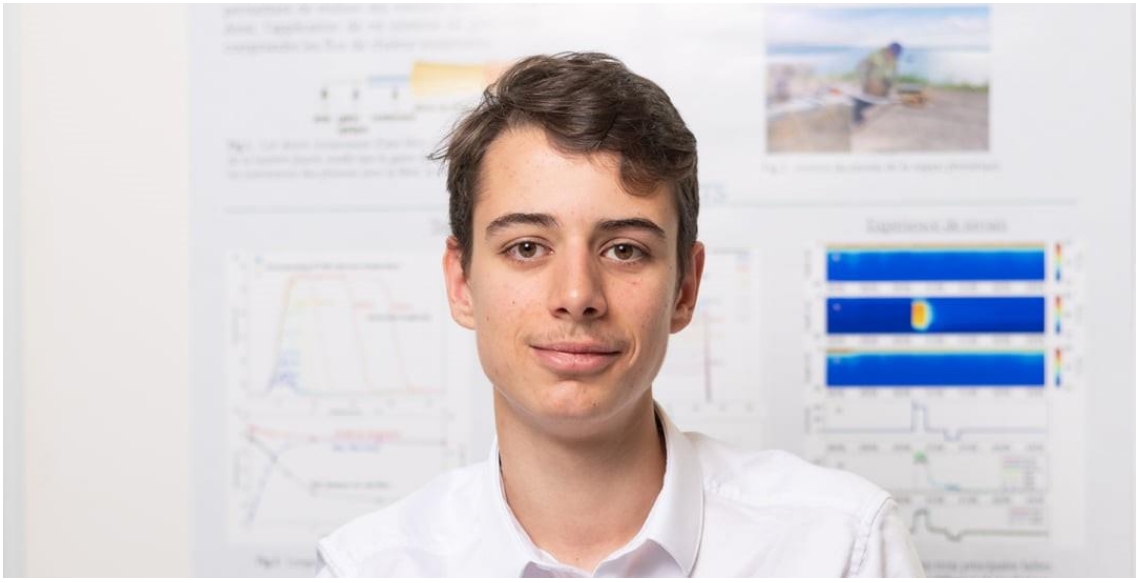

Summary

As part of the European project GEOTHERMICA - ERA NET and in order to assess the capacity of heat storage in Switzerland, the Centre d'Hydrogéologie et de Géothermie de l'Université de Neuchâtel (CHYN) is taking part in the HEATSTORE project, launched in 2018. The latter is expected to lead to commercial heat storage projects in the near future in Geneva and Bern, in fractured aquifers. The evaluation of the geological characteristics of these aquifers is essential to understand the thermal energy transport processes of fractured aquifers.

For this, it is necessary to be able to measure the temperature distribution along boreholes. Thus, the study focuses on the evaluation of a distributed temperature system (DTS) and its optical fiber in order to determine its operation, limits and potential for use in geothermal energy.

Laboratory and field tests have been carried out that the water temperature deviation measurements, with a scan time of 30 s, are reliable at less than 0.5°C at +/-5 m over 500 m of fiber. For absolute temperature values, however, a bath and a reference probe must be used to recalculate the absolute temperature to within 0.5°C.

The acquired data are essential for a broader understanding of the locations of fractured and karstified aquifers at Concise, allowing the system to be used to better understand the potential for water storage at a depth of 45°C at 35 m.

Personal Experience and Acknowledgements

In the first place, this Work made me discover and understand several issues related to geothermal but also allowed me a much broader personal development (and made me understand issues that were not directly related to the theme). First, I was able to learn the beginnings of programming languages such as Matlab, but also work tools like Overleaf or Adobe Illustrator, commonly used by scientists. The complementarity of laboratory and field experiments is essential: organization, practical problems, a notebook of experience, the concentration necessary not to lose the thread, etc. But the experience was mostly human: I learned to cooperate with a team and learn from them in a research environment.

Thus this program allowed me to discover a very different way of working, for which theoretical knowledge is no longer always sufficient, but requires knowing how to question, put into practice, dare to try and sometimes make mistakes. The academic framework also allowed me to understand what higher education looks like, as well as research and field experimentation involving several days of preparation.

In a word, I will always remember this unique moment that allowed me a real and profound personal development.

That is why I would like to thank my supervisors at the University of Neuchâtel at the Centre d'Hydrogéologie et de Géothermie (CHYN) and all the people I met there. An immense thank you for the warm welcome of Professor Dr Benoît Valley and Dr Reza Sohrabi, who accompanied me throughout this work and transmitted their passion for scientific research, especially geothermal. They have always been able to advise me, to push me to adopt a scientific approach, to make me think about the various problems and issues, and have always been available and attentive. I would also like to thank Mr. Laurent Marguet, who has always been very helpful during the difficulties encountered, whether in the field or in the laboratory. Thanks to them for their great patience and constant encouragement (*Fig.1)*.

Fig.1: Field data analysis © Sohrabi.

Many thanks to Mr Nicolas Paul, for his Physics lessons during these three years which I had the honor to attend. Thanks to Mr Christophe Jaberg, who made this exchange with the University possible.

Finally, I would like to thank my parents, for the countless proofreading, encouragement, and for their continued support and interest in my school career, and in particular this Mature Work.

1. Introduction

1.1. CLIMATE, MAN AND ENERGY

On a fragile planet, the Earth, where man must prevent too much climate disruption and preserve biodiversity, it is essential that the use of energy be rethought and sustainable. It is painful to project oneself into a world where scientific research and progress would not have made it possible to activate an important transition to cleaner energies and accessible in sufficient quantities to all, as advocated in the UN Sustainable Development Goals (UN, 2021)..

From the beginning of the industrial revolution until today, fossil fuels, which regenerate only over millions of years, such as coal, oil and gas are too heavily used; 84% of global primary consumption in 2019 (bp, 2021) is fossil and contributes significantly to greenhouse gas emissions, known to alter the climate.

For example, the sixth report of the Intergovernmental Panel on Climate Change states that "It is *unequivocal that human influence has warmed the atmosphere, ocean and land." (IPCC, 2021)*(IPCC, 2021)

Renewable energy, mainly hydro, solar and wind, accounted for only 11% of global primary consumption in 2019 (bp, 2021). Through research and development, they can become viable, local and more consistent solutions to global warming problems. Geothermal energy can produce electricity, heat and store energy locally. Already, the evolution of these energies is fast growing and will have to accompany a more eco-responsible consumption.

1.2. THE GEOTHERMAL

From the Greek «gêo», the Earth, and «thermos», heat, geothermal means the renewable energy coming from the thermal phenomena of the Earth's grounds, allowing the use of heat or the generation of electricity. Thus, the great advantages of this energy are that (1) it does not depend on climatic conditions and therefore allows the production of a constant and predictable ribbon energy, and (2) it is a local energy source independent of geopolitical hazards.

Indeed, the earth happens to be a gigantic reservoir of heat, while the temperature of the first meters of the ground is impacted by the climatic conditions, it is enough to drill beyond 10 to 20 meters so that the temperature of the ground no longer depends on the weather, Or the season. It will then increase with depth, depending on the type of subsoil and the depth, which is called the geothermal gradient *(Fig.2)*.

The Swiss plateau is essentially a sedimentary basin (green curve *Fig.2*), where the temperature increases by an average of 3°C every 100 meters. Geothermal installations must take into account geological conditions in order to determine their energy potential. In order to make the best use of the latter, different types of systems can be used.

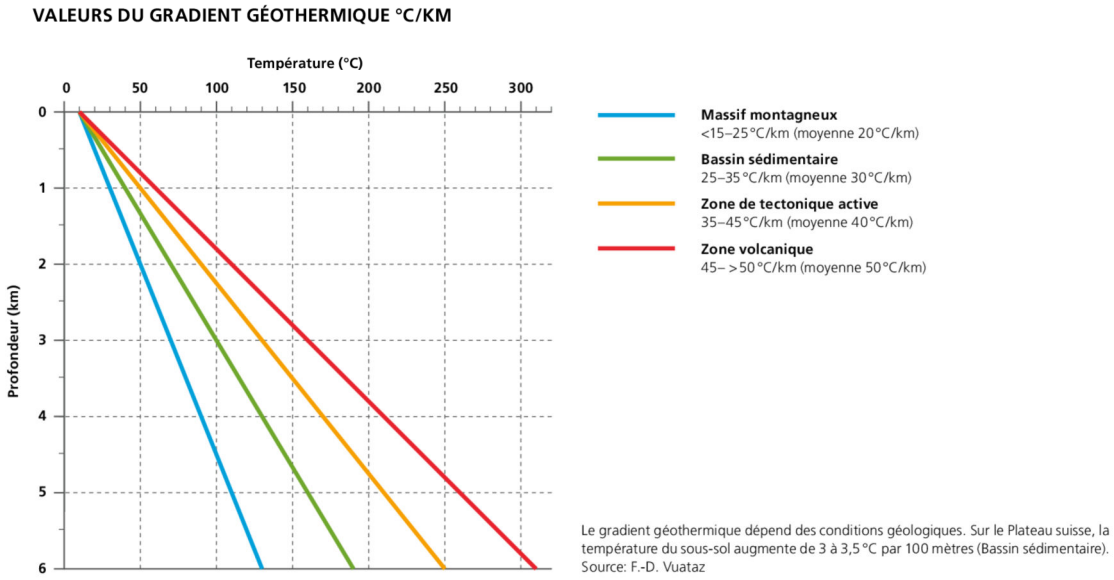

Fig.2: Typical geothermal gradients by subsurface (SuisseEnergie 2017)..

There are three main types of geothermal energy (*Fig.3):*

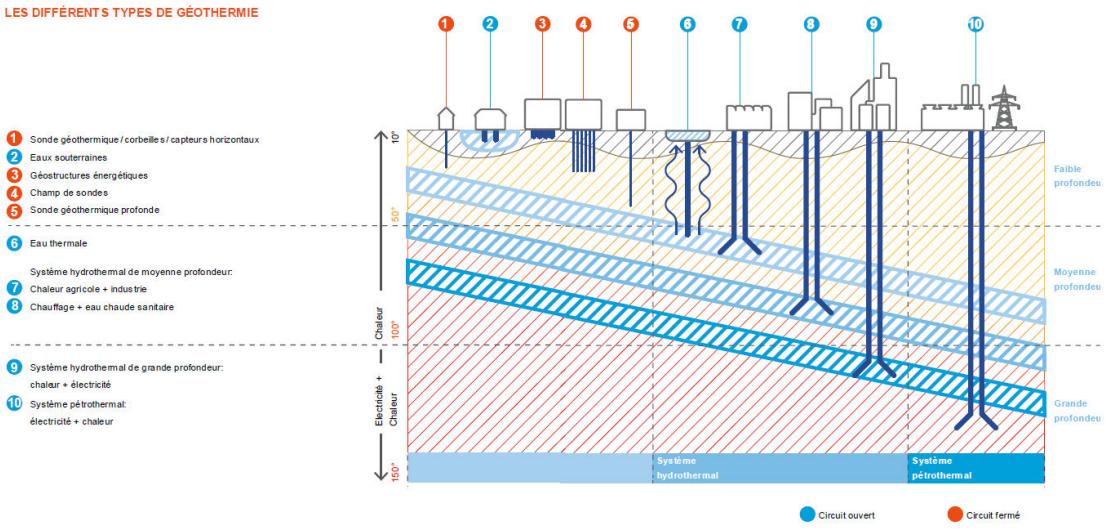

Fig.3: Major geothermal systems (SuisseEnergie, 2017).

Low-depth geothermal energy (numbers 1 to 5 in *Fig.3*) presents itself as an opportunity to provide energy to be consumed locally, mainly for heating. By one or more boreholes, groundwater is directly used for heating (in winter) and cooling (in summer) buildings. Indeed, it is enough to reach a shallow water table (100 to 200 m) for the water exploited to have a stable temperature throughout the year. This type of drilling is open drilling: the water in the subsoil is used as a heat vector.

Closed circuits use a coolant, which conveys energy. The cold fluid is injected into vertical geothermal probes (SGV, *Fig.4),* with a large heat exchange surface to increase the temperature of the fluid.

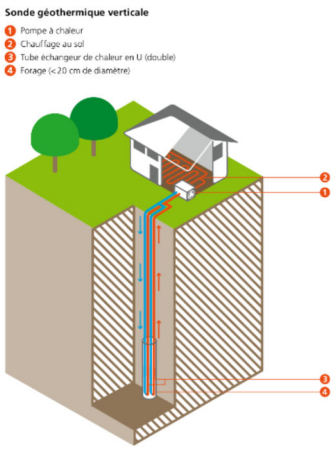

Fig.4: Vertical geothermal probes (Switzerland Energy, 2017).

Medium depth geothermal (numbers 6 to 8 in *Fig.3*) operates in an open circuit and allows a greater heat production than low depth geothermal. It is used for heating a group of buildings and for agricultural or industrial purposes most of the time. Recovered water typically reaches 50 to 100°C and drilling can range from 500 to 3000 m deep.

Finally, to create electricity, it is necessary to obtain water at a temperature above 100°C. Two systems are possible:

The first, called the deep hydrothermal system (number 9 in *Fig.3),* takes direct advantage of the fluids present in deep aquifers to start a turbine and an electricity generator, and to produce heat.

The second, called the deep petrothermal system (number 10 in *Fig.3)* or Enhanced Geothermal System (Fig.5), takes advantage of crystalline rocks whose permeability is increased by hydraulic stimulation: a fluid is injected to create or enlarge cracks, creating a cracked thermal reservoir. However, this process induces small microseisms, mostly not felt by the local population, although some of them reached between 3 and 3.9 magnitude on the Richter scale, in Basel and St.Gall. As Switzerland experiences a dozen equivalent natural seismic shocks each year, these artificial tremors are considered minor. However, it is important to warn the public. The acceptance of this type of project is difficult and we must therefore communicate in a transparent manner.

In addition to electricity, some deep systems use waste heat for district heating, so the heat source must be as close as possible to industrial centers, or buildings.

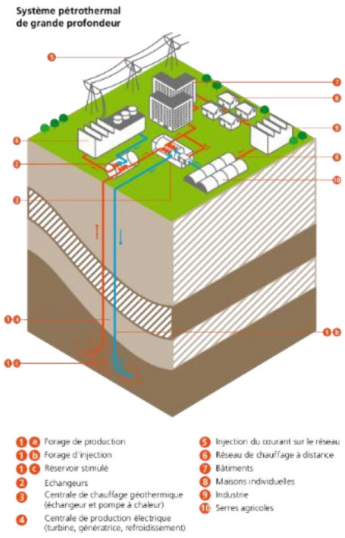

Fig.5: Enhanced Geothermal System (SuisseEnergie, 2017).

The costs of subsurface exploration are a very significant part of the final costs of a geothermal facility. Little is known about the subsoil in Switzerland because little oil or gas research has been done there. In addition, exploration remains highly random, and a site may prove to be unprofitable while the investment has been substantial. Finally, in order to develop all platforms in Switzerland more efficiently, drilling regulations should be harmonized at the federal level.

Although geothermal has some risks, it has many benefits:

- It is green, with stable and continuous production
- Switzerland can gain autonomy in its electricity supply.
- If the residual heat from deep boreholes is used, its price is competitive (*Fig.6)*.

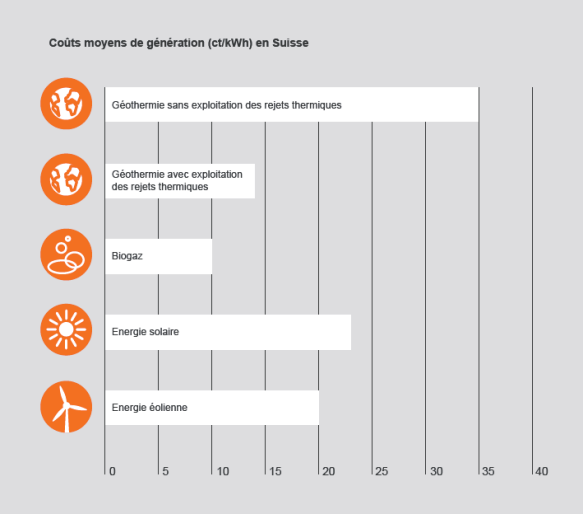

Fig.6: Average costs (in cents/kWh) for renewable energy sources (TA-SWISS, 2015).

1.3. HEAT TRANSFER IN AQUIFERS

"An aquifer is a geological formation containing temporarily or permanently movable water, consisting of permeable rocks, capable of naturally restoring it and/or by exploitation." (FuturaSciences, 2021) Saturated areas are distinguished when the interstices are filled with water from unsaturated areas where air is also present.

Three types of aquifers are distinguished:

1. Porous aquifers, such as gravel, allowing homogeneous movement of water, and reliable modelling of the system;
2. Fractured aquifers, such as granite, with cracks;
3. Karstified aquifers, such as limestone, including cavities.

These last two media are the most common in Switzerland: water flows – and therefore heat transport – are heterogeneous.

Heat transfer in aquifers depends mainly on two physical mechanisms:

1. Conduction, related to the existence of a temperature gradient; and
2. Advection, related to the presence of an underground flow.

Conduction characterizes the diffusion of heat between atoms by thermal gradient, without macroscopic motion of matter.

It is formalized by Fourier's law:

$$q = -\lambda \frac{\Delta T}{\Delta Z} \qquad (1)$$

With q heat flux (W/m2[2]), thermal conductivity (W/m/K), andλ T/$\Delta Z\Delta$ *temperature variation with depth (°C/m or K/m).* la variation de température avec la profondeur (°C/m ou K/m).

The thermal conductivity of air is 0.024, water is 0.6, and granite is 3.5 W/m/K. Soil conductivity depends essentially on three factors: the proportion of mineralogical constituents, porosity and water content. Since the air is very insulating, water-saturated soil will have a much higher thermal conductivity than dry soil (*Fig.7).*

Soil type	Thermal conductivity λ (W/m/K)	
	Dry	Saturated
Clay	0.2 – 0.3	1.1 – 1.6
Gravel	0.3 – 0.4	1.8 – 3.3

Fig. 7: Thermal conductivity of soils according to their water content.

Advection characterizes the underground flow, or the propagation of heat at the same rate as the medium in which it is located.

For a geothermal heating system, soils with high thermal power, that is to say with high thermal conductivity and high flow rate, will be sought (CFMS, 2017).

However, for geothermal storage facilities, the aquifer is not used as an energy resource, but as a means of storing thermal energy. For this reason and in contrast to heating systems, floors with low thermal conductivity and low flow rate to conserve heat will be sought (Le-Bel L. & Ungerer P., 2006).

1.4. HEAT STORAGE

The stored energy (in J) is the heat contained in the water. It is calculated as follows:

$$E = \rho \, C \, v \, \Delta T \qquad (2)$$

With$C$ mass *heat capacity (J/kg/K), and* ρ density (kg/m3), volume of water (m3v, le volume d'eau (m), temperature difference (K)ΔT, l'écart de température (K)

The mass heat capacity (or mass heat) of water is 4180 J/kg/K, with a density of 1000 kg/m3[3]. In a composite environment such as a water-saturated aquifer, the volume heat capacity of the aquifer will depend on the volumes occupied by the fluid and the solid respectively. (Courtois N. & al., 2007)

It is possible to use the underground aquifer to store this heat. It is therefore possible to inject high temperature water in summer (for example from an incineration plant). This heat would be recovered in winter by pumping the hot water stored in the ground and re-injecting it into a second well of water that has become cold (once the heat has been extracted). This system is in the research phase (HEATSTORE, 2021) and would allow to heat infrastructures in winter but also to cool buildings in summer (free-cooling) with cold water stored in aquifers. This principle has already been used and approved in Holland in porous aquifers, mainly gravel.

The three types of aquifers are being studied as part of the European research project HEATSTORE. In Switzerland, three sites were selected, each contributing to the understanding of a specific type of aquifer. The Centre d'Hydrogéologie et de Géothermie (CHYN), at the University of Neuchâtel, is in charge of experiments at the Concise site (*Fig.8)* (in the canton of Vaud around Lake Neuchâtel).

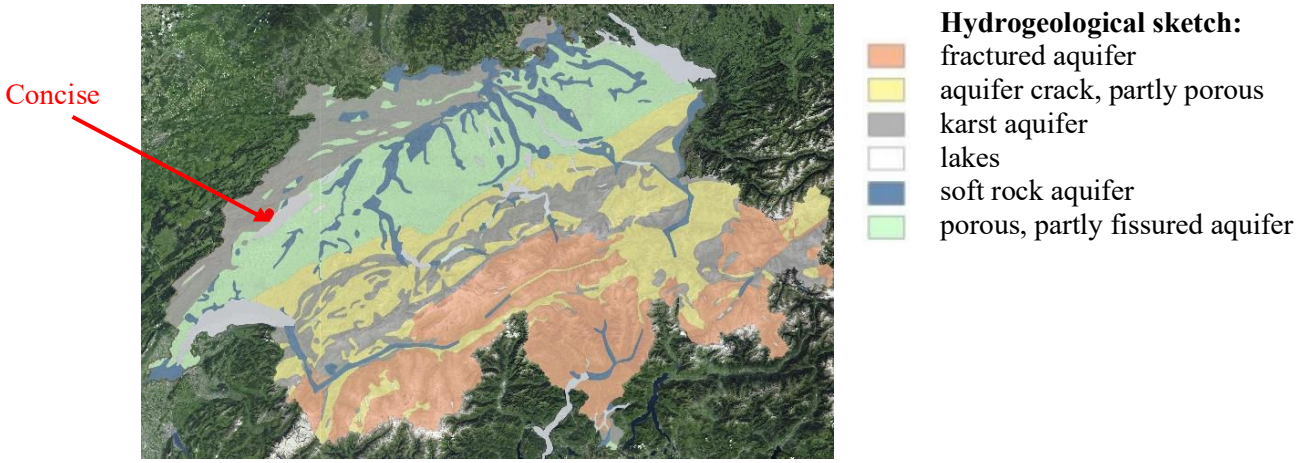

Fig.8: Hydrogeological sketch and geographical position of Concise (Swiss Confederation, 2021).

1.5. STUDY OBJECTIVES: MEASUREMENT SYSTEM

The objective of this research is to evaluate and understand the operation of a fiber-optic distributed temperature measurement (DTS) system (*Fig.9)*.

The laboratory tests will allow to understand the operation of the configurations and the calibration of the fiber, as well as to define the accuracy of the measurement system.

The field tests will test the system in real applications, to better understand the distribution of fractures in the drilling, and after processing the data, to be able to explain in more detail the way heat exchanges are conducted in the aquifer concerned. At Concise, the studied aquifer is fractured and karstified.

This study also aims to propose a protocol for the installation of the device and analysis of DTS data to facilitate the future deployment of the system in other boreholes.

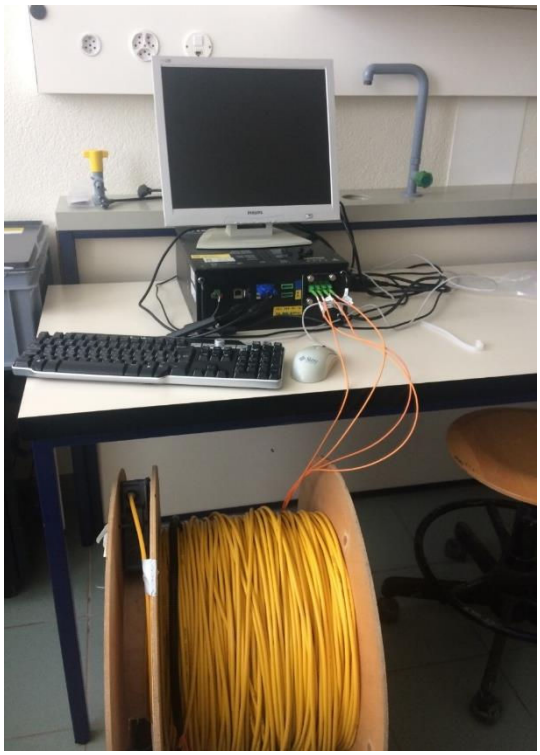

Fig.9: DTS Sentry with 500 meters of fiber optic © Posta.

2. Qualification of Laboratory Measuring Equipment

In this chapter, we will describe the main devices, such as the DTS (Temperature Sensing, Measure) sentinel (ORYX+ XR15) and the optical fiber (ULTRA-FOX PLUS), as well as their functions. These tools are used together in order to measure temperatures as a function of a distance, that is to say at several points, which differentiates it from a conventional thermometer that only takes spot measurements of temperature. The sentry emits a laser at one end of the fiber, before receiving it from the other end. The laser travelling through the core of the fiber loses virtually no energy thanks to the phenomenon of total internal reflection. But the photons emitted interact differently in the fiber, depending on the temperature of the inner matter (very influenced by the outer one). In this way, the sentry can determine a temperature profile along the fiber. Second, we will explain the experimental devices put in place to evaluate this temperature measurement system.

2.1. FIBER OPTIC & SENTINEL DTS

Optical fiber is a light wave guide, usually used for the transmission of high-speed information. It *is used as a geothermal temperature sensor in boreholes, thanks to a temperature-dependent reflected wavelength. The fiber is composed of several layers (*Fig.10) to confine and preserve the light – and therefore the information – and is composed of a soul (also called the heart) which is the physical support of the light, an optical sheath for reflection and then a series of coatings and reinforcements.

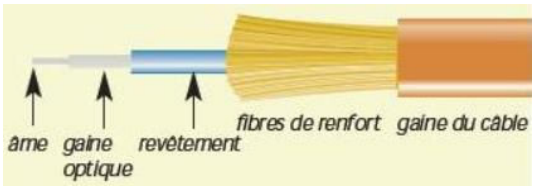

Fig.10: Photograph of different parts of the fiber (Blackbox, 2021).

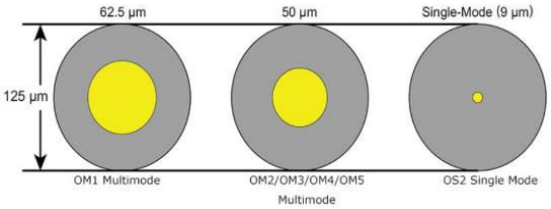

Fig.11: Representation of fiber optic core diameters (Blackbox, 2021).

Our fiber is type «OM2 50/125 µm Multimode» (*Fig.11)*, which means that it has a core of 50 micrometers and a sheath of 125 micrometers. The term multimode means that several light rays (or modes) can travel at the same time in this soul. In addition, the optical fiber forms a loop: two channels actually form a single fiber segment, their ends being connected to the end of the fiber. Finally, to respect the minimum radius of curvature of the fiber (*Fig.12)* there is a housing at the end of it. Here is the main information about fiber optics (*Fig.12):*

Number of channels/loops	Minimum radius of curvature	Type of fiber
#4 / #2	9.6 cm in installation and 6.5 cm in operation	OM2 50/125 µm Multimode

Fig.12: Fiber data (Sensornet, YellowCableSpecs, 2010).

The DTS sentry (*Fig.13)* is an opto-electronic instrument, connected to the fiber with an E-2000 connector. The device provides temperature measurements for negative distances (zero at the E-2000 connector). This is because the DTS sentry has about 50 meters of fiber inside. After starting the sentry, it will emit optical pulses, travelling in the heart of the optical fiber, but will also play the role of receiver

of information. The system is designed by the manufacturer as having a temperature resolution depending on the scan time and fiber length. In our case, the measurements are averaged generally for 30 seconds and the fiber measures 510 m (+ 50 m in the sentinel), the accuracy of the measurement should be 1 sigma = 0.15°C (*Fig.14)*.

Here is the main information about the sentry (*Fig.15*), more information about the device descriptions can be found in the respective datasheets. These two tools were designed by the English company Sensornet.

Fig.13: Photograph of the DTS sentry used (Sensornet, DataSheet v.2, 2020).

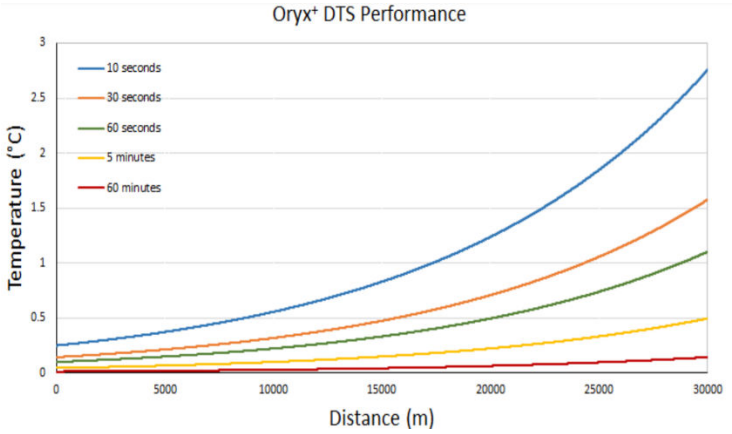

Fig.14: Graph representing the accuracy of the Temperature as a function of the acquisition time of the measurement and the length of the fiber used (accuracy of +/ 1 sigma = 68% probability) (Sensornet, DataSheet v.2, 2020).

Resolution spatial	Temperature resolution	Minimum duration of measurement time	Laser pulse wavelength
1.02 m	0.004°C	10 secs	1550 nm (infrared)

Fig.15: DTS Sentry data (Sensornet, DataSheet v.2, 2020).

2.1.1 Physical principles of Fiber optics

To ensure the containment of the incident light (emitted by the laser) and to avoid energy losses, the optical fiber uses the refractive properties of the core and the optical sheath. The index of refraction, called$n$, is defined for a given medium by the ratio of *c* the velocity of light in vacuum, *to l* the velocity of light in this medium (Avianzi P. & al., 2007)*:*

$$n = \frac{c}{l} \qquad (3)$$

Snell-Descartes' second equation for refraction is expressed as (Giancoli D., 2004):

$$n_1 \sin\theta_i = n_2 \sin\theta_1 \qquad (4)$$

Where the angleθ_i is the angle of the incident light,θ_1 is the angle of the refracted light and wheren_1 & n_2 are the refractive indices of their respective environments.

The third equation of Snell-Descartes concerns reflection, such as (Avianzi P. & al., 2007):

$$\theta_i = \theta_r \qquad (5)$$

Whereθ_r is the angle of the reflected light (*Fig.16)*.

From equation (4), we can derive the value of the angleθ_c which defines the critical angle of the incident light below which the internal reflection is total, that is, there is no more light loss (and therefore that$\theta_1 =$ 90°):

$$sin\,\theta_c = \frac{n_2}{n_1} \qquad (6)$$

So$n_1 > n_2$: the refractive index of the heartn_1 must be higher than that of the sheathn_2.

This is also why we must respect the minimum radius of curvature of the fiber, so that the energy of the ray is reflected, otherwise the optical signals, containing the information, would be refracted out of the heart and would be lost.

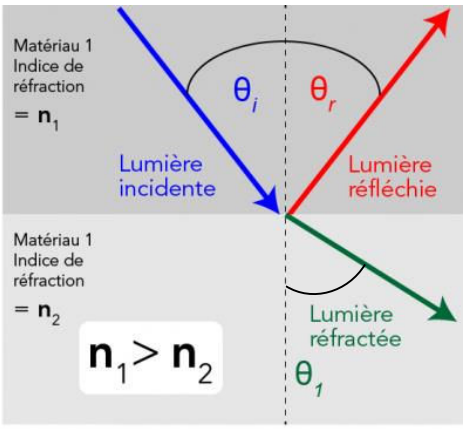

Fig. 16: Illustration of reflection and refraction (Let's Talk Science, 2021)..

2.1.2 Physical Principles of the SDR Sentinel

Temperature is the macroscopic reflection of the agitation of molecules and atoms of matter.

The Energy Level allows to define the quantum states that can take an atom: at each energy level corresponds a particular state of the system. The energy levels of the electron layers of an atom make it possible to predict the absorption or emission spectrum of photons (Wikipedia Raman scattering, 2021).

Diffusion is called inelastic when the energy brought by the incident radiation is different from that of the scattered radiation. The Stokes process is the fact that the photon loses energy - by the emission of a phonon - and the Anti-Stokes process if not - by the absorption of a phonon - (*Fig.17)*.

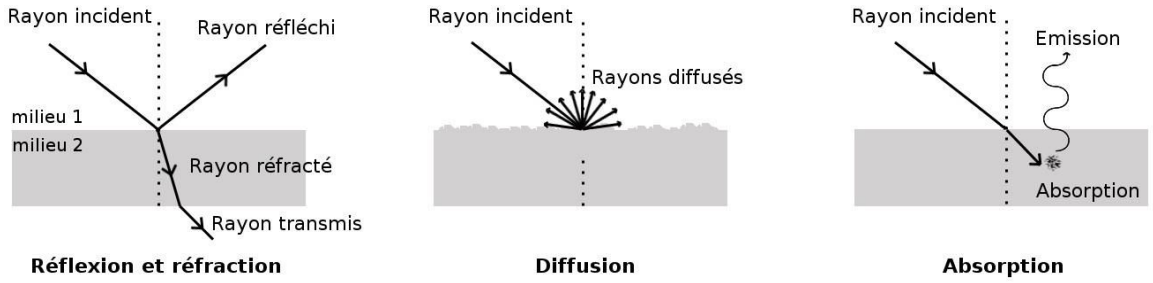

Fig.17: Illustration of the differences between reflection, refraction (macroscopic level), Diffusion and absorption (microscopic level) (Clenet 2012).

In order to measure a temperature change of the optical fiber, and therefore of its medium, the sentinel DTS emits photons (optical pulse), these will have a probability of being part of the absorption spectrum of atoms constituting the core of the fiber (depending on energy levels). If the photon energy is absorbed by the electrons (in the form of vibrational transition energy), the energy level increases before returning to normal either through a Stokes or Anti-Stokes process. But most of the time, the scattered photon will have kept the same energy, it is said that the diffusion is elastic (*Fig.18).*

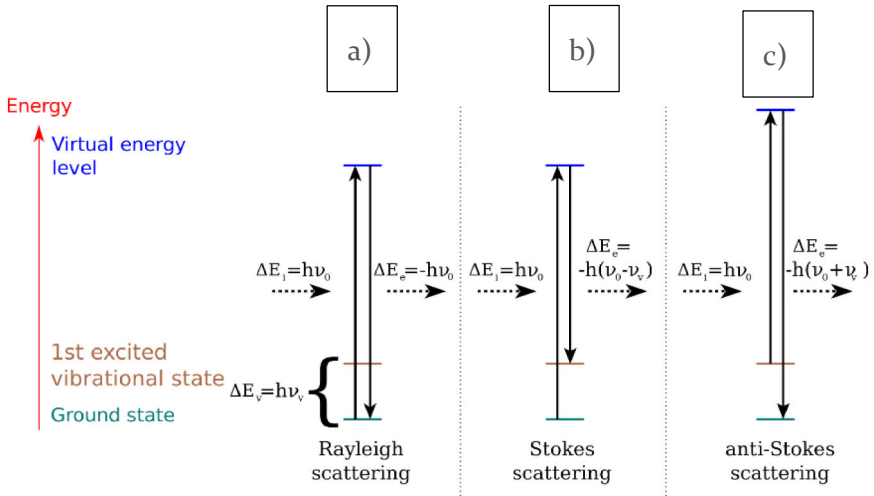

Fig.18: a) Elastic diffusion or Rayleigh. b) Inelastic diffusion (Stokes), c) Inelastic Diffusion (Anti-Stokes) (CC BY-SA 3.0, 2021).

The energy, calledE , transported by a photon can be calculated using the Planck-Einstein equation (Commissions romandes de mathématiques, 2018):

$$E = h\,v = h\,\frac{c}{\lambda} = h\,c\,\vartheta \qquad (7)$$

Where$h$ is the Planck constant equal to 6.63*10-34^{-34} J.s, v is the frequency in Hz,c is the speed of light in vacuum in m/s,λ is the wavelength in m, andϑ is the number of waves inm^{-1} .

Thus the optical pulse will be subjected to two main types of radiation scattering (*Fig.19):*

1. Rayleigh Diffusion is an elastic diffusion, that is, kinetic energy is conserved, but the direction of particle propagation is changed. This process is therefore random and cannot provide information on the measurements, but it is useful for the calibration of the device because it is the most present diffusion.

2. Raman Scattering is an inelastic scattering, the energy brought by the incident radiation will be different from that of the scattered radiation.

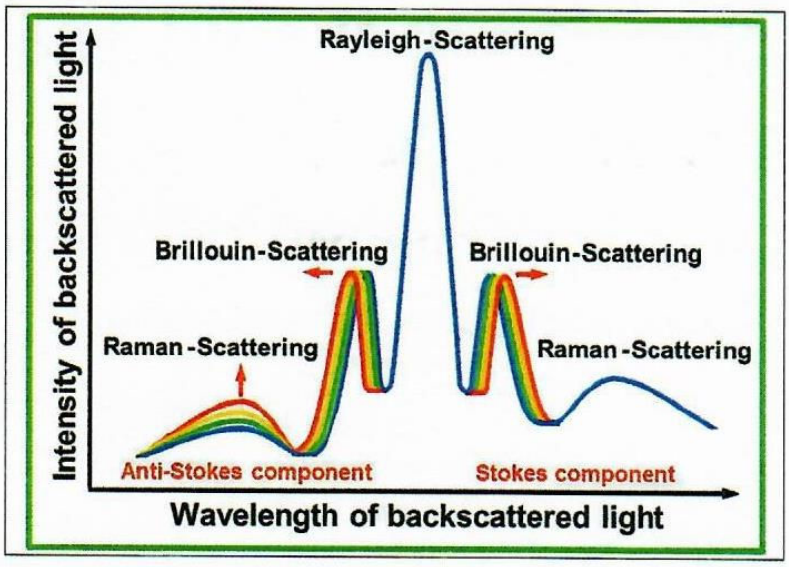

Fig.19: Illustration of release types (Buecker C. & Grosswig S., 2017).

Finally, the device determines the anti-stoke and stoke intensities that take place according to the time separating the optical emission from its return (thus the distance travelled):

1. The Anti-Stokes and Stokes intensities allow the temperature to be calculated using the following formula:

$$\frac{I_a}{I_s} = \frac{(\vartheta_0 + \vartheta_k)^4}{(\vartheta_0 - \vartheta_k)^4} \, exp^{\left(\frac{-h\, l\, \vartheta_0}{k\, T}\right)} \quad (8)$$

Where I_a represents the intensity of Anti-stokes, I_s the intensity of Stokes, ϑ_0 the number of waves of incident light (in m^{-1}), ϑ_k the amount of offset of the number of waves (in m^{-1}), h the Planck constant (6.63*10-34^{-34} J.s), l the speed of light in the optical fiber (in m/s), k Boltzmann constant (1.38*10-23^{-23} J/K) and T temperature (in K).

2. The time between the emission and the reception of the photons makes it possible to define the distance at which this temperature is measured, knowing that a photon travels about 1 m in 10 ns (depends on the refractive index, cf. Eq. [3]).

2.1.3 DTS Sentinel Configuration and Data Processing with Matlab

Before starting an experiment, we configure the DTS sentinel, for this it is essential to make an initial acquisition of the data, on which we can apply manual corrections. First, it is necessary to indicate the length of the loops (that is to say twice the length of the fiber, since a loop goes back and forth in the fiber) so that the sentinel only recovers the information that will be necessary to us (without noise before and

after). Then we configure the acquisition time of the measurements which influences their accuracy (as shown in *Fig. 14)*, and finally the frequency of repetition of the measurements.

To improve the accuracy of the measurements, which is the combined effect of accuracy and precision, we process the data acquired by the DTS sentinel with Matlab. Matlab is a computational computer language used for this Work.

It is necessary to calibrate the temperature (*Fig.21)* at the different points of the fiber, with a reference probe. To do this, a thermometer (PT100) is placed in the reference bath with the fiber during the experiments.

Since the principle of measurement is based on measurements of amplitudes, attenuation (the loss of amplitude when light travels along the fiber) influences the measurement. This results in an apparent increase in temperature with the measuring distance. It is an artifact that needs to be corrected.

This adjustment was made on Matlab in the following way: during the experiments, a reference bath (a cooler filled with water at room temperature, the water helps to limit too volatile fluctuations in temperature) is positioned at the beginning of fiber (20^{th} to 30^{th} meters). Since the fiber is made of a loop, two measurements of the same temperature (that of the reference bath water) are made (Fig.20). Thus the two segments which must have the same temperature allow to calculate and correct this slope. This improves the accuracy of the measurement.

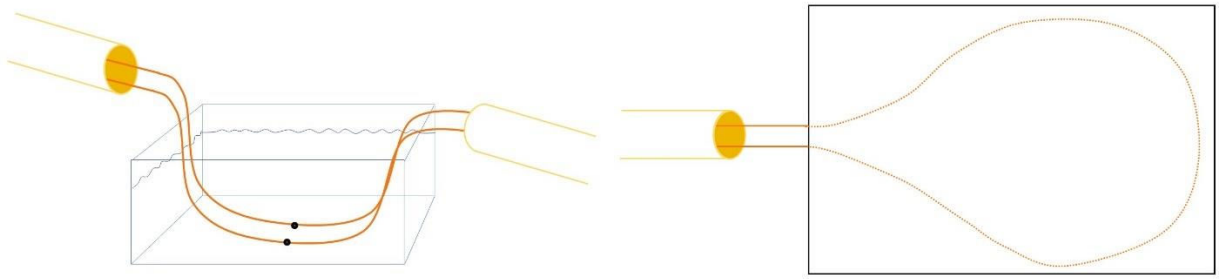

Fig.20: On the left, two measurements of the same temperature by the loop. On the right, loop formed in the black case at the end of the yellow cable.

Then, the set of data is adjusted by a vertical translation equal to the difference between the temperature given by the fiber and that measured by the thermometer (*Fig.21).* This improves the accuracy of the measurement.

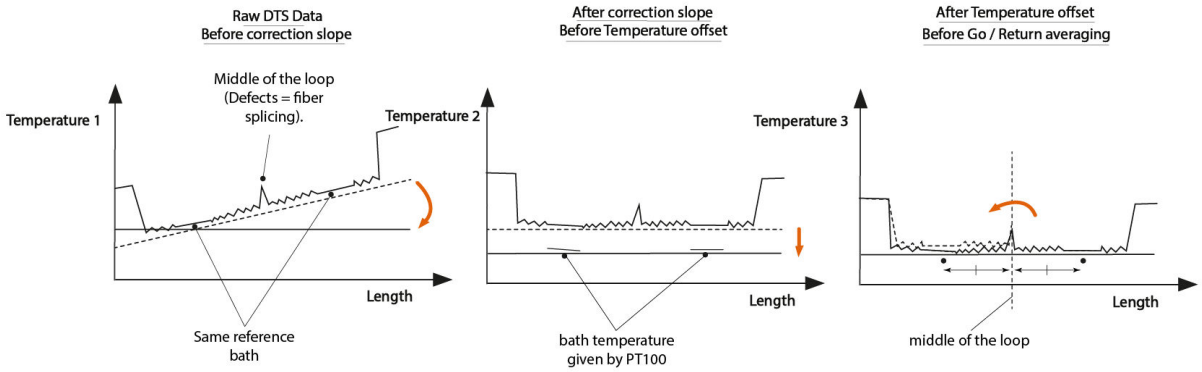

Fig.21: Calibration of "The Slope Correction" and "The Temperature Offset".

2.2 EQUIPMENT, INSTALLATION AND METHODS

2.2.1 General Equipment and Installation

- A computer screen
- 1 foehn
- One DTS Sentry (ORYX+XR15)
- Optical fiber (ULTRA-FOX PLUS)
- The 2 PT100 (temperature probes)
- 1 USB key
- 1 computer (for data analysis)
- 1 roll of Adhesive Tape
- Two coolers (30 cm x 40 cm x 40 cm to respect the minimum radius of curvature of the fiber) and their insulating covers
- 48 liters of hot water (50°C max.), provide kettles if the tap does not rise to 50°C
- 48 liters of water at room temperature (23 to 24°C)

During the experiments, the general installation was as follows:

- Connect the DTS Sentry to the mains
- Connect the optical fiber (Channel 1 with Loop1 – A, Channel 2 with Loop 1 – B, Channel 3 with Loop2 – A, Channel 4 with Loop 2 -B), the 2 PT100 and the display.
- Fill the first cooler with water at room temperature (cooler #1 or reference bath), place the PT100 #1 on it, then close with its thermal cover to avoid random temperature fluctuations.
- Fill the second cooler with hot water (cooler #2), place the PT100 #2 in the cooler, then close the cooler with its thermal cover to avoid heat loss.
- Use scotch to keep the fiber in the coolers during experiments.
- Start data taking on DTS with 60 sec scan time and frequency.
- Heat the fiber slightly with the foehn, to highlight the heated place on the graphics.
- Be careful not to overwrite or touch the fiber especially during data capture.
- Use a USB key at the end of the experiments to transfer the data to a computer (analysis on Matlab).

2.2.2 Effect of Submerged Length

After following the general installation, we placed 10 m of fiber in cooler #1 (reference bath) from the 20th to the 30th meter of fiber from the E-2000 connector. We used the foehn to highlight the entry and exit points of the cooler fiber. Then we plunged 0.1 m of fiber into cooler #2, we waited four minutes to ensure that the submerged fiber segment reached the actual temperature value. Finally, we repeated the manoeuvre for lengths of 0.2 m, 0.4 m, 0.6 m, 1 m, 2 m, 3 m, 5 m, 10 m, and 15 m. This experiment must determine the minimum length that must be submerged for the temperature resolution to be satisfactory. (Experiment carried out on 10 August, from 12.25 to 14.00)

2.2.3 Effect of Scan Time per Measurement

Four DTS Sentry configurations have been created. Only the scan time was changed successively to 10 sec, 20 sec, 30 sec, 60 sec. Seven measurements (seven times the scan time of each configuration) were performed. The accuracy of the temperature can be compared between each configuration and will help define the most appropriate acquisition time for field experiments. (Experiment carried out on August 10, from 14:12 to 14:28).

Note: This experiment is carried out after the experiment *2.2.2 Effect of the submerged length,* we use its final installation.

2.3 LABORATORY ANALYSIS AND RESULTS

Important note for the reading and understanding of the graphs: the color variations represent time, they begin with dark blue, then gradually degrade to green, yellow, and finally to dark red. Thus, the blue curves indicate the start of the experiment, while the red curves are the end of the experiment.

2.3.1 Effect of Submerged Length

Only the relevant curves were used to show the response of the fiber temperature measurement for each submerged length (Fig. 22, the lines correspond to the temperatures measured by the fiber). We averaged the last two measurements (out of a total of four) for each submerged length. It is evident from this figure that the temperature measured by the fiber is much too low when only a short section of fiber is submerged. This is illustrated in more detail in Fig.22 where the maximum measured temperature has been extracted for each length of submerged fiber. This allows a comparison with the measured temperature with the PT100. The black curve represents this temperature difference. Note that a logarithmic scale is used to the right of the graph.

Finally, we were able to deduce from this experiment that it is necessary to use at least 10 meters of fiber to ensure that the real value of the temperature (formation of a significant «plateau») is measured. In fact, the DTS measures the intensity over a duration corresponding to a length of fiber.

5 meters of fiber may suffice but the bias is -0.7°C while it is only -0.45°C with 10 meters (*Fig.22)*; moreover, there is no improvement when 15 meters of fiber are used.

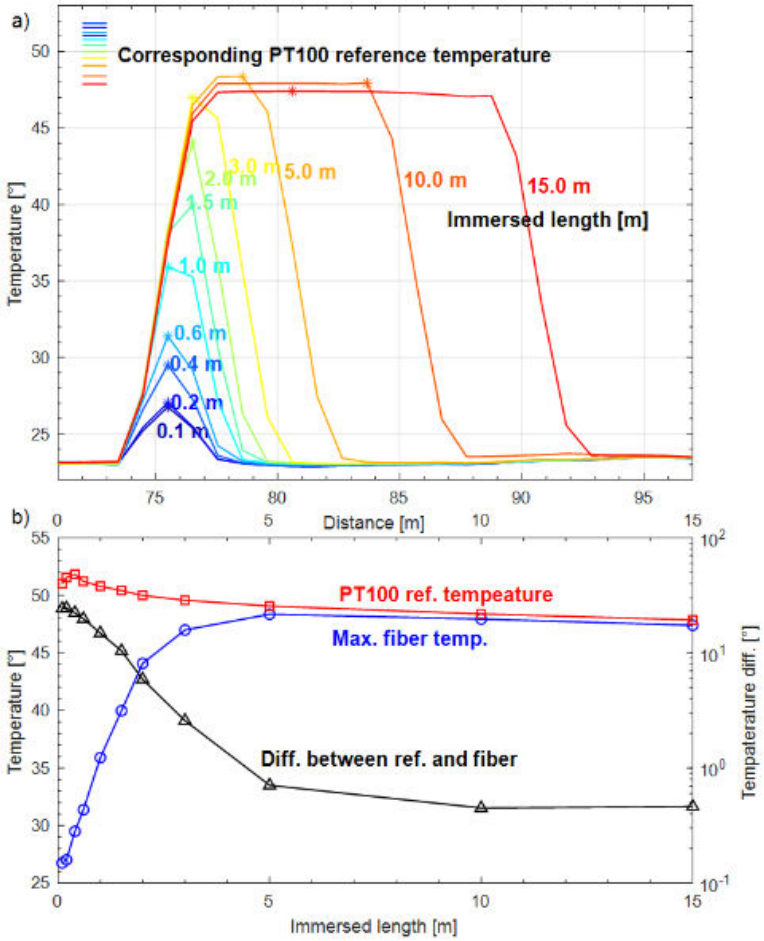

Fig.22: a) Temperatures measured by the fiber according to the length of the submerged fiber, b) Comparison of measured temperatures between PT100 probe and fiber.

2.3.2 Effect of Scan Time per Measurement

Seven measurements per configuration were performed by changing the scan time to 10, 20, 30 and 60 seconds. The results after processing on Matlab are presented in Fig.23 *As* the total scan time increases, there is an increasing temperature drop due to heat loss.

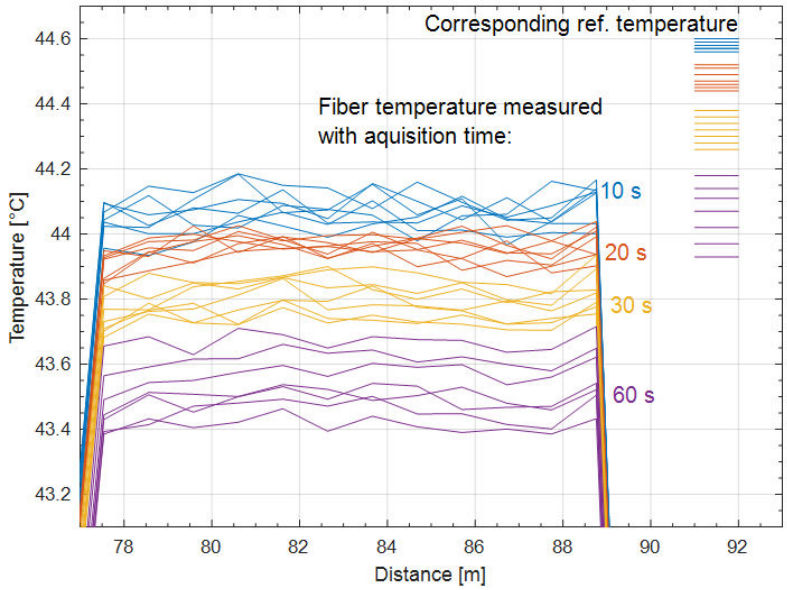

Fig.23: Temperature measured by fiber as a function of scan time.

We selected 8 points distributed regularly every 1.02 m along the submerged segment (between 79.56 and 87.72 m), we use the values of these eight points for the 7 successive measurements of each configuration, we then obtain clouds of 56 points for which we calculated (1) median bias with PT100 and (2) interquartile deviation (IQR interquartile). The results are presented in *Fig.24.* We observe a sharp decrease in the interquartile deviation and thus an improvement in the accuracy of the measurement from 30 seconds of acquisition.

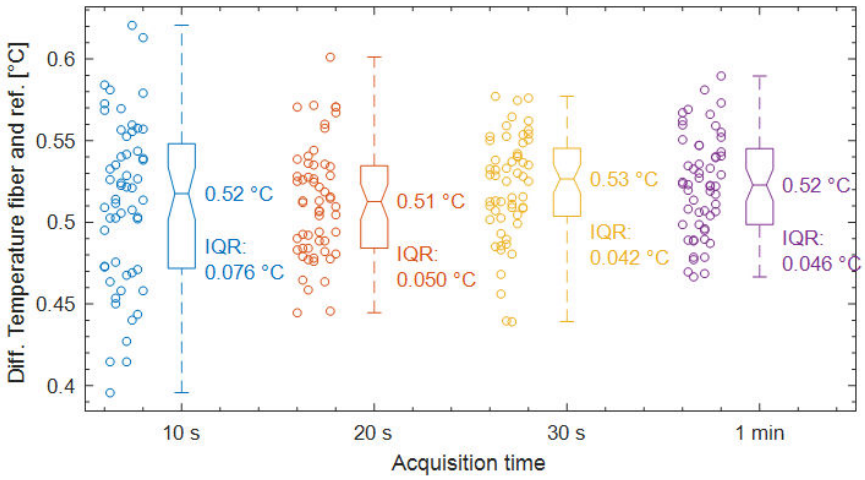

Fig.24: Whisker boxes and temperature difference between PT100 probe and fiber.

3 Application of measurement equipment in the field

3.1 HARDWARE, INSTALLATION AND WORKFLOW

In this chapter, we describe the field measurements, carried out seven days in a row around Concise (VD). The experiment involved three 50 m deep vertical wells forming an equilateral 4.5 m triangle. This site was chosen for its hydrogeological characteristics as seen above. The aim is to understand the means of diffusion of hot water between boreholes. To do that, we injected hot water into a well, and then we analyzed the impact on the other two wells.

Although the diffusion of hot water was minimal, the temperatures quickly returned to normal as soon as the injection stopped. This experiment highlights a high underground flow rate (advection) and the presence of three faults in the well (at 12, 20 and 30 meters depth). We conclude that the place is not suitable for heat storage.

3.1.1 Hardware and Installation

- All laboratory equipment with one cooler (see *2.2.1)*
- Water (~22 $m3^3$) that was brought from a hydrant pump through pipes to the boilers
- 2 boilers for hot water injection at a total flow rate of 40 l/min at 50°C
- 1 water table pump (15 l/min)
- 1 Water table height detection piezometric probe
- 3 Keller (Pressure and Temperature) and 3 RBR (Temperature) probes
- 1 probe for logging (logger) (measurement of rock characteristics including temperature measurement)
- 3 empty PET bottles (or any container with a diameter between 6.5 cm and 11.5 cm) to respect the bend radius of the fiber
- Multiple 12 V or 24 V batteries if it is not possible to connect to the mains
- Petrol for pumps
- SDR and screen protections to allow the facility to take measurements during nights

The DTS Sentry is configured with a 30 second Acquisition Time, a 1090.38 m Range, and a 1.001 Stokes Length Correction.

During the experiment,

- Connect the DTS sentry to the mains in a nearby house, connect the fiber optic, both PT100 and the display.
- Fill the cooler with water at room temperature, place a PT100, ~15 m of fiber optic, then close with a thermal cover.
- Keep the fiber in the cooler with the scotch during experiments.
- Be careful not to overwrite or touch the fiber especially during data capture. Unroll the fiber, prepare 3 loops of 2x50 m, each weighted with a bottle filled with gravel, and install a loop in each well (*Fig.25).*
- Twice immerse ~15 m of fiber in the cooler (reference bath) between wells 2 and 3 and after well 3.

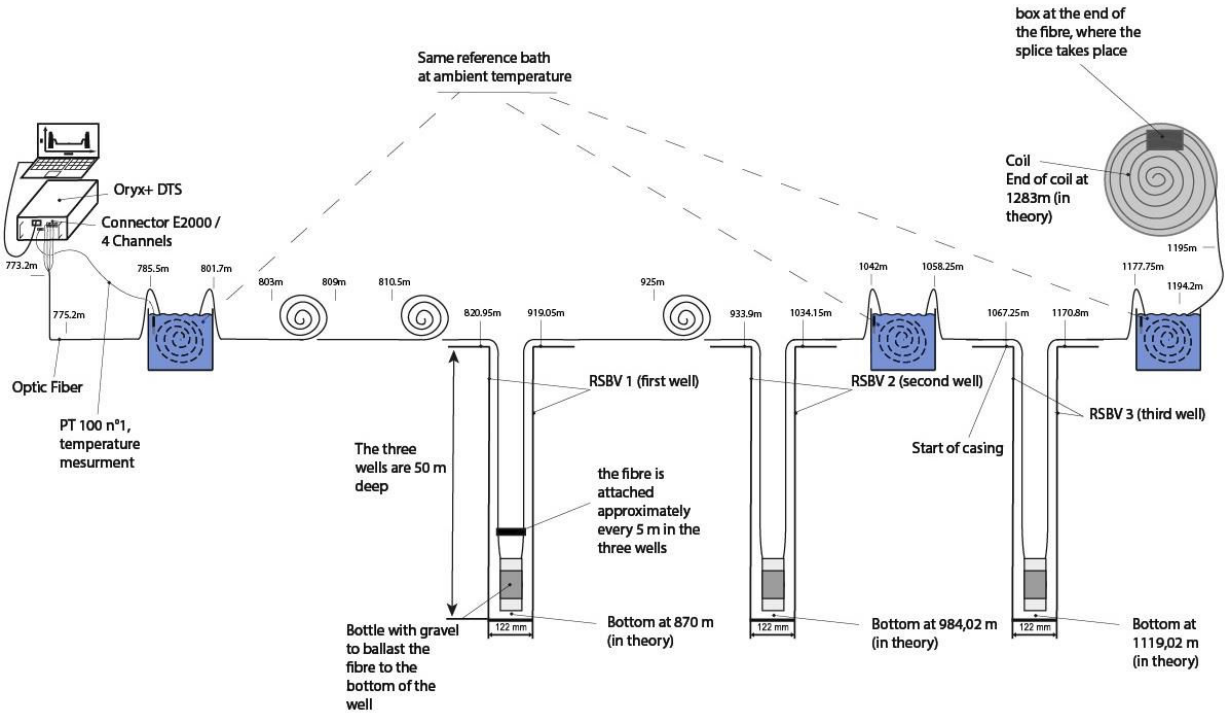

Fig.25: Fiber device for field measurements.

3.1.2 Unfolding

Aug 27	Well logging (checking strata of each well), Fiber unrolling and distance marking (see *Fig.25),* Preparation of fiber ballast bottles and placement of fiber in bottles, Installation of RBR temperature probes at 35 m depth, and Keller pressure probes at 45m depth, Start the DTS sentry in early afternoon, start measurements.
August 28 and 29	Rest of the wells, the disturbances created by the opening of the wells and the insertion of the fibers in the boreholes are thus stabilized, Passive monitoring to ensure the experiment runs smoothly.
Aug 30	Hot water injection into the RSBV-2 well at approximately 45°C with a flow rate of 40 l/min for 9 hours, Regular verification of the temperature of the water injected from the boilers, Regular check of the water table height with a piezometric probe.
Aug 31	Water table pumping from the RSBV-2 well with a flow of 15 l/min for 9 hours.
September 1 to Sept 3	Passive monitoring, Disassembly.

Fig.26: Logbook of the field.

3.2 FIELD RESULTS

The overall result of the measurement sequence is shown in *Fig.26*.

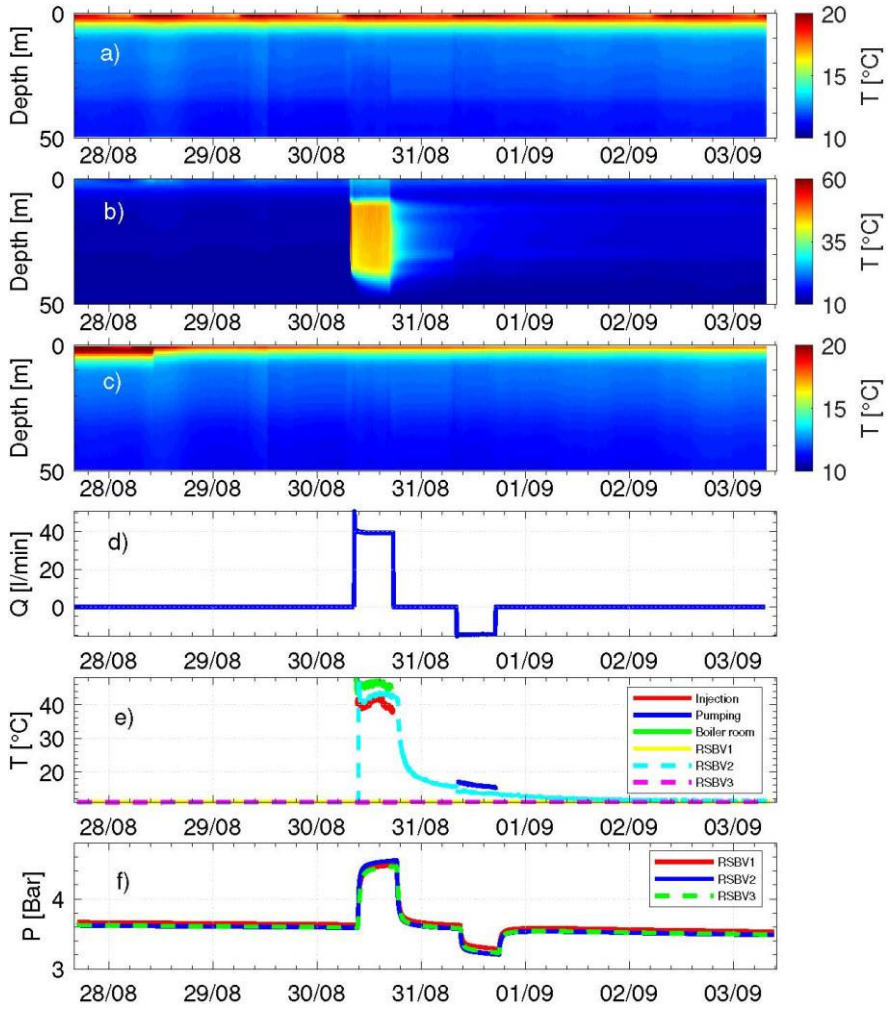

Fig.26: Time is recorded in UTC. For a), b) and c) the color variations represent the different temperatures inside the drill according to the optical fiber. a) drilling temperature RSBV-1 as a function of time and depth. b) drilling temperature RSBV-2 as a function of time and depth. c) RSBV-3 drilling temperature as a function of time and depth. d) Volume injected and pumped into RSBV-2 drilling during the experiment. e) Temperature of the three wells, as well as the water injected and pumped during the experiment. f) Height of the water table in the three wells, represented by the pressure captured by a probe at a depth of 45 m (Keller), representation during the experiment (Sohrabi R. & Valley B., Overview of the August 2021 heating test in Concise, 2021).

In *a)* and *c)* we notice that the temperature fluctuates slightly over time above -33 meters. We think these fluctuations are created by the difference in air temperature between day and night on the water temperature in the boreholes. Well *c)* being closer to the hill, it shows slightly lower temperatures than well *a)* downstream, or the temperatures happen to be slightly higher.

The fault at -30 m would be mainly influenced by the flow of water, but during the injection of hot water, the latter was still able to highlight the fault, where the flow is not large enough.

The temperature of the water measured at 15 l/min is only 15°C while that injected is about 45°C, so the water injected has diluted with water at 11.5°C or is gone.

3.2.1 Analysis before hot water injection

We note in *Fig. 27* that the temperature of the water in the rest boreholes varies from 10.9°C to 12.5°C. The higher temperatures, shown in white, highlight areas without water or too much influenced by external conditions. The two troughs appearing around noon could be explained by a warming of the air, which is in direct contact with the water. But this increase affects the entire length of the drilling and seems too sudden. Measurements made with the fiber at 22 m, 35 m or 45 m everywhere undergo the same reaction. The break from August 29 at noon is also far too strong. In addition, the RBR temperature probes placed at 35 m in each well prove that the temperature is constant. The temperature indicated by the DTS sentry appears to decrease overall over time. The bias is approximately the same in the 3 wells, it is at the beginning of +0.6°C and at the end of +0.4°C. The precision seems difficult to qualify because it would be for $1\sigma \cong 0.05°C$ over a very short interval but from 0.25 to 0.3°C over the entire duration of the experiment. These variations will probably turn out to be artifacts, being present only by a default of configuration or processing, but the exact source is currently unknown. Comparison with reference bath data as well as air temperature data may be relevant. It may also be interesting to verify in the laboratory that the same problem does not appear when the experimental bath (cooler #2) has a temperature of 10°C instead of 50°C. The distance differences tested should also be similar to those in the field, and the use of BRR could replace PT100 in the laboratory.

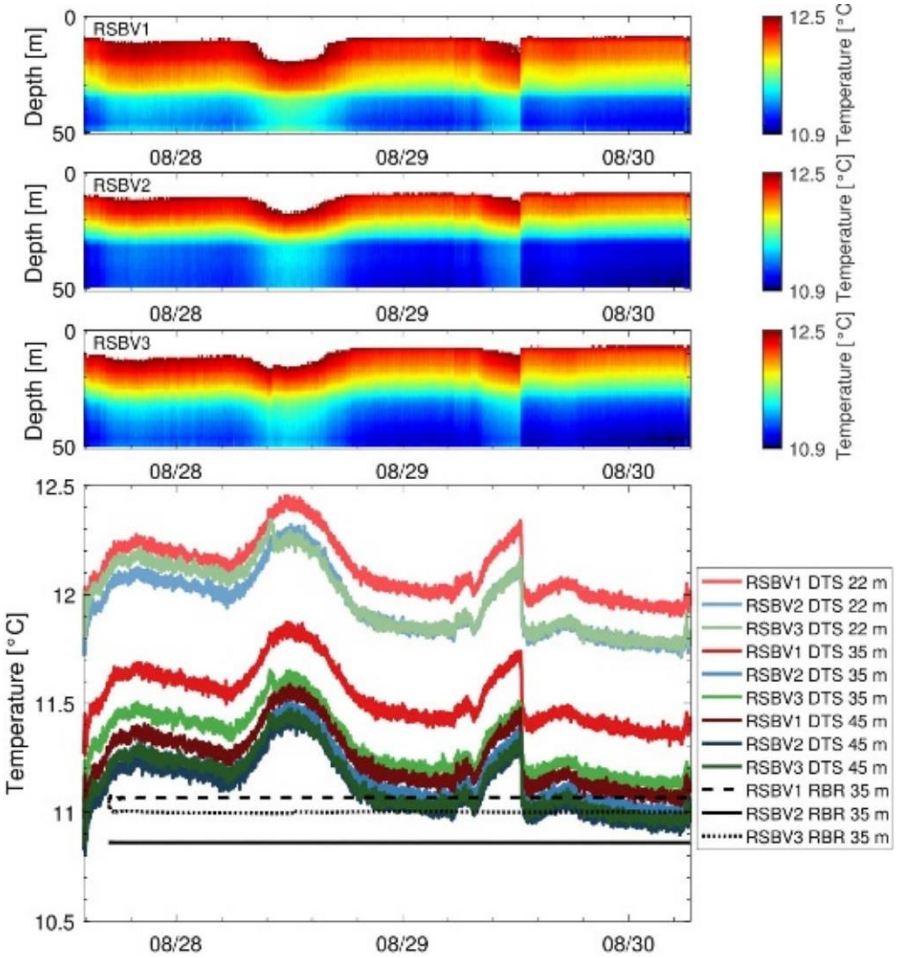

Fig.27: Temperatures before hot water injection. Top: thermal maps representing values between 10.9 and 12.5°C for RSBV1, RSBV2 and RSBV3, respectively. Out of range data is shown in white.
At the bottom: temperature curves, based on DTS sentinel data and RBR temperature probe data, for defined depths.
(Sohrabi R. & Valley B., Overview of the August 2021 heating test in Concise, 2021)

We compare on Fig.28 the data of the DTS sentinel with those of the log. We find that the change of environment (and therefore of the coefficient of heat exchange) seems to play an important role on the log

while no sudden change is visible for the SDR. Since logging takes almost two hours to complete and this was done first in well #1 then #2 then #3, we can explain that the temperatures of well #2 and 3 logging are lower by -2 to -18 m than in well #1: The probe just out of drill hole 1 did not have time to warm up to room temperature before being reused in the second drill hole. Although some subtleties visible on the log are not represented on the DTS (due to the difference in spatial resolutions), the overall shape of the curves is identical in the saturated area. DTS temperatures are generally 0.3°C warmer than logging temperatures.

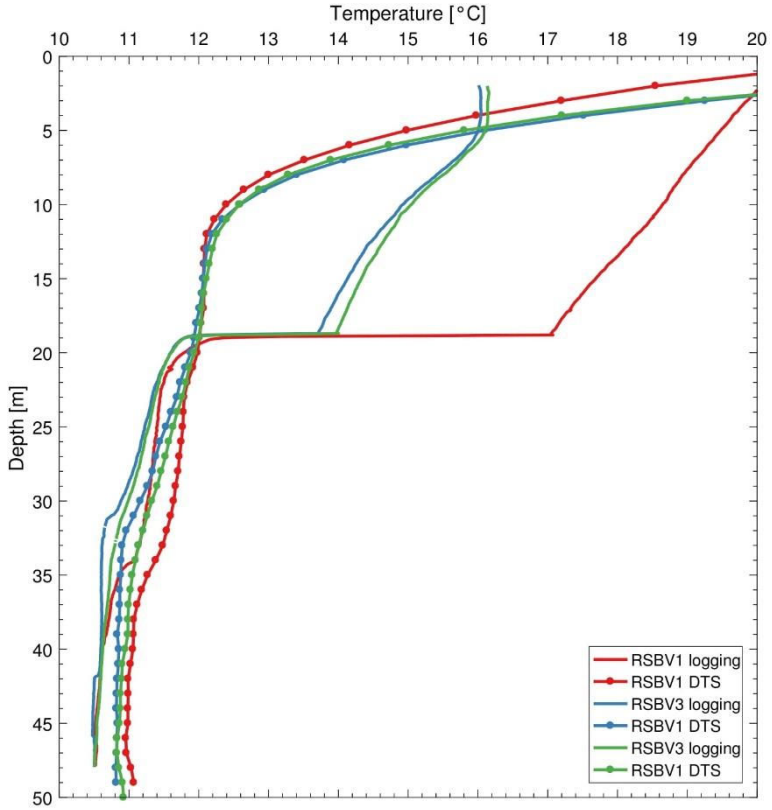

Fig.28: Comparison of data acquired during the day of August 28, 2021 (RSBV1 at 08:56, RSBV2 at 10:56, RSBV3 at 12:43 UTC logging end hours) with DTS data acquired in the boreholes on August 28, 2021 at 14:11 UTC. (Sohrabi R. & Valley B., Overview of the August 2021 heating test in Concise, 2021).

3.2.2 Analysis after hot water injection

Although the injection of hot water at 45°C into the RSBV-2 well lasted 9 hours, the temperature of wells 1 and 3 (observation boreholes) did not change very much during the experiment. Nevertheless, the pressure of these boreholes (and thus the level of their groundwater) followed spontaneously without any marked latency. The injected water would then “push” the water already present in the aquifer (cooler than that in contact with outside air) before bringing it into the other two boreholes. This explains why a very slight decrease in temperature affects the observation boreholes at the beginning of the injection.

In RSBV-2, we can notice that once after injecting hot water, the heat dissipation is not identical and forms curves. We can notice three "bumps" where the heat takes longer to cool down, these reveal the position of the main faults along the drilling: the hot water could be stored in greater quantities during the injection and when this stops, the faults stay warm longer. We notice here three main faults, one at -11.5 m, at -19.5 m and at -30 m. We can also notice that below about -43 m, the injected water does not heat much the sub-Water flows from the surrounding heights, carrying the heat by advection. In the other two boreholes, the temperature remains more stable below -43 m than above because the flowing water is less impacted by the higher air temperature.

The advance of the hot water front is illustrated in Fig.29. The hot water injection began at 0725 at a temperature of 60°C for about 10 minutes before descending to a temperature of 45°C, the injection temperature for the remaining 9 hours. Fig.29 a) shows the temperatures at the start of the injection, which quickly reach 59°C in the drilling (Fig.29 b). the temperature is distributed well over the whole depth of the drill but a clear break is visible from -38 m where a large fractured zone is located.

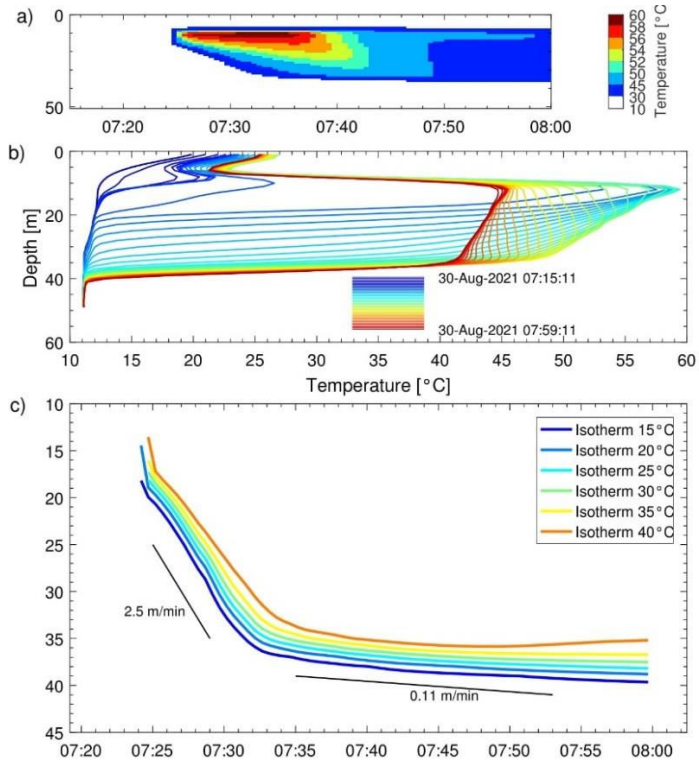

Fig.29. Illustrations of the advance of the heat front in borehole RSBV-2 during hot water injection. a) Thermal map in drill hole RSBV-2 at start of hot water injection. b) Successive temperature projections in RSBV-2 during hot water injection. c) Estimation of the speed of advance of the hot water front along the borehole and as a function of time: (Sohrabi R. & Valley B., Overview of the August 2021 heating test in Concise, 2021).

4 Conclusion and Outlook

4.1 CONCLUSION

During this work, I used a DTS system as well as an optical fiber as a temperature detection medium to understand the heat movements in the underground. Indeed, thanks to the Raman anti-Stokes and Stokes diffusions over time, it is possible to determine a temperature profile along the fiber. I finally defined a protocol for optimal use of the device.

It was on this basis that I assessed the measurement system by characterizing the limits and capabilities of the device in the laboratory. It takes at least 10 meters of fiber to reach a real value of temperature, and 30 seconds of scan time to optimize our future field experiments and an accuracy of around 0.5°C over the 500 meters of fiber. On the other hand, field experience has made it possible to understand the means of heat diffusion at the site of Concise (VD), where advection is important, and to experiment with measuring instruments on a wider scale. The DTS system allows a simpler management of the measuring device, because once installed it does not have to be changed. The system also allows for a greater production of measurements and these are less impacted by the thermal conductivity of the measured medium than by using a log.

4.2 OUTLOOK

In order to determine even more precisely the capabilities of the DTS (Distributed Temperature Sensing) technology, we could have carried out experiments on different optical fibers, Check that slope and bias corrections are similar at temperatures between 10 and 60°C… Especially to better understand the mysterious breakouts of the order of 0.3°C appearing every midis.

The DTS system is a very useful tool for measuring in space and time geothermal phenomena in the field.

Ultimately, this measurement system is necessary to assess the geothermal potential of a region and allows a better understanding of the distribution of subsurface temperatures. Also, the measurement tool studied allows the competent authorities to be better informed about energy efficiency and helps to make the right choices when it comes to an investment for a geothermal installation.

Bibliography

Avianzi P. & al. (2007). *Physics 4* (Vol. 4). L.E.P.

Bandweaver. (2020). *Distributed Temperature Sensing – DTS.* Retrieved from https://www.bandweaver.com/fiber_optic_sensing_technology/distributed-temperature-sensing/

Blackbox. (2021, 08). Retrieved from https://www.blackbox.en/en/page/27220/Information/Technique/black-box-explique/Cables-fiber-optique/constitution-dun-cble-fiber-optique

bp. (2021). *Statistical Review of World Energy.* Retrieved from https://www.bp.com/en/global/corporate/energy-economics/statistical-review-of-world-energy.html

Buecker C. & Grosswig S. (2017). Distributed temperature sensing in the oil and gas industry - insights and perspectives. *Oil Gas European Magazine*, 9.

CC BY-SA 3.0. (2021). *Wikipedia Diffusion Raman*. Retrieved from https://en.wikipedia.org/wiki/Diffusion_Raman

CFMS. (2017). *Recommendations for the design, sizing and implementation of geothermal thermal structures.* French Committee for Soil Mechanics and Geotechnical Engineering. Retrieved from https://www.geotechnique-journal.org/articles/geotech/abs/2016/04/geotech170012s/geotech170012s.html

Clenet, H. (2012). Retrieved from http://harold-clenet.com/site/wp-content/uploads/2012/07/Fig_b_Interac_milieu.jpg

Commissions romandes de mathématiques, d. p. (2018). *Formulaires et Tables.*

ConfederationSwitzerland. (2021). Hydrogeological sketch. Retrieved from https://map.geo.admin.ch/

Courtois N. & al. (2007). *Application of thermal storage in aquifers to the heating and cooling of vegetable greenhouses in France: pre-feasibility study. Report BRGM/RP55481-EN Retrieved from https://www.ademe.fr/sites/default/files/assets/documents/55373_stockage_thermiqueaquifere_ure_serres_rapport.pdf* Rapport BRGM/RP55481-FR. Récupéré sur https://www.ademe.fr/sites/default/files/assets/documents/55373_stockage_thermiqueaquifere_ure_serres_rapport.pdf

FuturaSciences. (2021). *Aquifer.* Retrieved from https://www.futura-sciences.com/planete/definitions/geologie-aquifere-1030/

Giancoli D. (2004). *Physique Générale 3: Ondes, Optique et Physique moderne* (Vol. 3). (F. Gobeil, Trad.) de boeck.

Biotechnology Expert Group: Biochemistry-Biological Engineering Teachers, I.-I. e. (2013). *Metrology Resource Paper*. Retrieved from https://www.ac-strasbourg.fr/fileadmin/pedagogie/biotechnologies/Metrologie/Document_ressource_metrologie_octobre_2013.pdf

HEATSTORE. (2021). *www.heatstore.eu*. Retrieved from www.heatstore.eu

IPCC. (2021). *IPCC Sixth Assessment Report*. Retrieved from https://www.ipcc.ch/report/ar6/wg1

ISO-5725-1. (1994). Accuracy of measurement results and methods — Part 1: General principles and definitions. *Retrieved from https://www.iso.org/obp/ui/#iso:std:iso:5725:-1:ed-1:v1:en* Récupéré sur https://www.iso.org/obp/ui/#iso:std:iso:5725:-1:ed-1:v1:fr

ISO-5725-2. (2019). *Accuracy (accuracy) of measurement results and methods — Part 2: The basic method for determining the repeatability and reproducibility of a standardized measurement method.* Retrieved from https://www.iso.org/obp/ui/#iso:std:69419:en

JCGM-200. (2012). *International Metrology Vocabulary – Fundamental and General Concepts and Associated Terms (VIM) 3rd Edition.* Retrieved from https://www.bipm.org/en/publications/guides

Le-*Bel L. & Ungerer P. (2006).* Aquifer heat storage: a new perspective for geothermal energy. Mines Paris. Retrieved from https://www.mines-paris.org/global/gene/link.php?doc_id=1018&fg=1

Bonsprofs. (n.d.). *Snell-Descartes Act*. Retrieved from https://www.lesbonsprofs.com/espace/seconde/physique-chimie/ondes-et-signaux-1/2491/199227

UN. (2021, 08 18). Sustainable Development Goals. Retrieved from *www.un.org: www.un.org/sustainabledevelopment*. Récupéré sur www.un.org: www.un.org/sustainabledevelopment/fr/objectifs-de-developpement-durable

Let's Talk Science. (2021). Retrieved from https://parlonssciences.ca/ressources-pedagogiques/documents-dinformation/la-reflexion-et-la-refraction

Sci-Tech-Visa (2022) Retrieved from https://scitechvista.nat.gov.tw/Theme/C000004/detail?ID=a3c3a71c-dd1c-4af4-baad-9f38c8a70e9a

Sensornet. (2005). Senti*nel DTS User Manual.* Retrieved from https://www.sensornet.co.uk

Sensornet. (2010). YellowCableSpecs.

Sensornet. (2020). *DataSheet v.2.* Retrieved from https://www.sensornet.co.uk/wp-content/uploads/2020/01/Oryx-DTS-range-data-sheet-v2.pdf

Sohrabi R. & Valley B. (2020). *RSBV Borehole Hydrogeology* Report (Concise, Vaud). Centre d'Hydrogeoloogie et de Géothermie (CHYN), University of Neuchâtel.

Sohrabi R. & Valley B. (2021). *Overview of the August 2021 heating test in Concise.* Hydrogeology and Geothermal Centre of the University of Neuchâtel.

SuisseEnergie. (2017). *Geothermal in Switzerland. A versatile energy source.* SFOE.

TA-SWISS. (2015). *Electrical power from the ground.* Retrieved from https://www.ta-swiss.ch

Thermo Scientific Spectroscopy & Material Analysis. (2017). *Raman Spectroscopy, Stokes vs Anti-Stokes.* Retrieved from https://www.youtube.com/watch?v=zYVxsxphlJc

Stilld. (2021). *Metrological quality of a measuring device*. Retrieved from Wikipedia: https://commons.wikimedia.org/w/index.php?curid=80274297

Wikipedia Raman scattering. (2021, 10 9). Retrieved from https://en.wikipedia.org/wiki/Raman_scattering

【評語】180019

Innovative study of measuring temperature along the length of optic/laser fiber using light scattering principle，with good applications in geothermal profiling. Good understanding of the problem，the measurement principles/physics. Complete work with instrument calibration，field experiment and results reporting. In-depth reading of literature can carry the study further.